

SFE-O: An Optical Model for the San Francisco Estuary

Steven G. Ackleson and W. Joseph Rhea
Naval Research Laboratory, Washington, DC, USA

Sarah Blaser, Frances Wilkerson, and Richard Dugdale
San Francisco State University, CA, USA

Curtis O. Davis and Nick Tuffillaro
Oregon State University, OR, USA

1. INTRODUCTION

The San Francisco Estuary (SFE) is the largest estuary and wetland habitat on the Pacific Coast of the United States. It is an ecologically important system that links freshwater and marine environments, provides drinking water to over 25 million urban users, and irrigation water for agriculture in the highly productive Central Valley (Service, 2007). Ecological pressures are expected to intensify in the future with continued population increase (ABAG, 2015) and changes in climate (Cloern et al., 2011). The purpose of this work is to develop a constituent-based optical model (SFE-O) for the northern portion of the SFE, including the lower reaches of the Sacramento River and Delta, Suisun Bay, San Pablo Bay, and Central Bay (Fig. 1). We focus on data collected during two cruises of the region conducted in May 2014 and March 2015. Water inherent optical properties (absorption and scatter) were measured coincident with in-water and above-water radiometry and water sample collections. A total of 22 stations were occupied stretching from the Golden Gate to Sacramento. While the model is controlled by the rate of light absorption and scatter by the water mixture, the core of the model is focused on establishing transforms between the mass and optical properties of the primary water mixture constituents; phytoplankton, non-living particulate matter, and dissolved organic matter. The model is constructed based on statistical relationships between optical properties and constituent concentration measured within the study region and is tested against independent measurements of water reflectance and in-water light intensity.

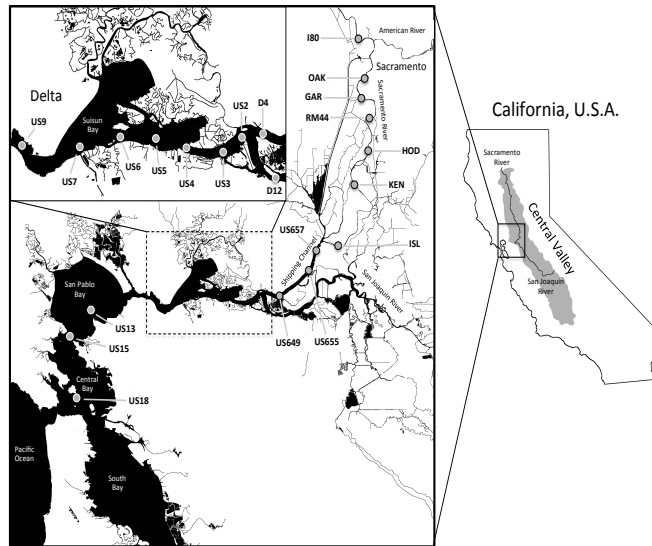


Figure 1. Study site setting and station locations.
The dashed box indicates Suisun Bay and lower reaches of the Sacramento River.

2. MODEL DESCRIPTION

The propagation of irradiance, $E \text{ Wm}^2$, through a body of water is controlled by the rate of absorption and volume scatter by the water mixture, expressed as coefficients $a \text{ m}^{-1}$ and $\beta \text{ m}^{-1}$, respectively. Integrating β across all possible scatter directions results in the total light scatter

coefficient, $b = 2\pi \int_0^\pi \beta(\theta, \phi) \sin\theta d\theta \text{ m}^{-1}$. Integrating β across a subset of angles results in the rate of light scatter into the corresponding direction. In remote sensing problems, the relevant scatter direction is backward, i.e., scatter of downwelling light back towards the surface: $b_b = 2\pi \int_{\frac{\pi}{2}}^\pi \beta(\theta, \phi) \sin\theta d\theta \text{ m}^{-1}$. The fractional backscatter, often employed in ocean radiative transfer models and ocean color remote sensing algorithms, is defined as $\tilde{b}_b = b_b/b$.

The optical properties, a and b , are partitioned linearly between the primary constituents of the water mixture:

$$a = a_w + a_{phy} + a_{SPM} + a_{CDOM} , \quad (1)$$

$$b = b_w + b_{phy} + b_{SPM} , \quad (2)$$

where the subscripts w , phy , SPM , and $CDOM$ refer to pure water, phytoplankton, non-living particles (e.g., detritus, silt and clay), and colored dissolved organic matter, respectively. The properties of pure water are considered constant and CDOM, being in dissolved form, only contributes to absorption.

Modeling a constituent optical property P require accounting for both magnitude and spectral response;

$$P = CP'\mathcal{F} , \quad (3)$$

where C represents constituent concentration, generally mass, P' is a constituent-specific, multiplicative factor that links constituent concentration to the magnitude of the optical effect, and \mathcal{F} is a dimensionless function that adjusts P spectrally relative to a reference wavelength, λ_0 nm. The formulation of C , P' , and \mathcal{F} depends on the constituent and the associated optical property.

Fractional backscatter, \tilde{b}_b , is not defined as a constituent-specific property. Instead, it is parameterized as a function of λ and applied to the total scattering coefficient, b . For modeling purposes, \tilde{b}_b is used to constrain β with an appropriate scattering phase function.

2.1 Phytoplankton

Phytoplankton absorption and scattering are formulated as:

$$a_{phy} = C_{chl} a'_{chl,675} \mathcal{F}_{a,phy} , \quad (4)$$

$$b_{phy} = C_{chl} b'_{chl,675} \mathcal{F}_{b,phy} , \quad (5)$$

where $C_{chl} \text{ mg m}^{-3}$ is chlorophyll a concentration and $a'_{chl} \text{ m}^2 \text{ mg}^{-1}$ and $b'_{chl} \text{ m}^2 \text{ mg}^{-1}$ are chlorophyll-specific absorption and scatter referenced to $\lambda_0 = 675 \text{ nm}$. The spectral factors, $\mathcal{F}_{a,phy}$ and $\mathcal{F}_{b,phy}$, are computed as the average of 16 marine phytoplankton species absorption and scatter spectra reported by Stramski et al. (2001) and normalized to $\lambda_0 = 675 \text{ nm}$. The average values for $a'_{chl,675}$ and $b'_{chl,675}$ are $0.013 \text{ m}^2 \text{ mg}^{-1}$ and $0.125 \text{ m}^2 \text{ mg}^{-1}$, respectively. The shape of

the adopted $\mathcal{F}_{a,phy}$ is most similar to the spectrum for coastal phytoplankton reported by Ciotti et al. (2002) representing "microplankton".

2.2 Non-Living Particulate Matter

Organic and inorganic particles are expected to have different absorption and scattering characteristics owing to differences in composition and particle size. Operationally, the optical properties of organic matter may be scaled to measured values of particulate organic carbon (POC) while inorganic properties are scaled to the mass of all non-organic particles in suspension. If the sources and transport mechanisms of the two particle types are similar, from a modeling perspective they could be grouped into a single, non-living particle constituent having combined absorption and scattering characteristics. The unique conditions of the SFE support such an optical grouping since the concentration of SPM, C_{SPM} g m⁻³, is driven primarily by current and wind suspension of bottom sediments (Schoellhamer, 2002) and wetlands within the Delta are the primary sources of POC (Müller-Solger et al., 2002). Simultaneous measurements of C_{SPM} and POC concentration within the SFE reveal a strong linear correlation between the two parameters (Murrell and Hollibaugh, 2000); N=49 and $r^2 = 0.76$. Therefore, for modeling simplicity, all non-living particulate matter is grouped into single absorption and scattering terms and referenced to C_{SPM} ;

$$a_{SPM} = C_{SPM} a'_{SPM,489} \mathcal{F}_{a,SPM}, \quad (6)$$

$$b_{SPM} = C_{SPM} b'_{SPM,652} \mathcal{F}_{b,SPM}. \quad (7)$$

SPM absorption is referenced to $\lambda_o = 489$ nm and scatter to $\lambda_o = 652$ nm. The SPM spectral shape function is of the form

$$\mathcal{F}_{a,SPM} = \sum_0^3 x_i [\lambda/\lambda_o]^i \quad (8)$$

for $400 \leq \lambda \leq 750$ nm. For $\lambda > 750$ nm, the bracketed term is constant $[750/\lambda_o]$. The spectral shape of SPM scatter is of the form

$$\mathcal{F}_{b,SPM} = [\lambda/\lambda_o]^{-\eta}. \quad (9)$$

The coefficient η is the spectral slope of $\ln[b_{SPM,\lambda}]$ versus λ . The coefficients x_0, x_1, x_2 , and x_3 and exponent η are derived empirically from field measurements.

2.3 CDOM

Absorption by CDOM is attributed to the presence of colored dissolved organic matter of biological origin (Jerlov, 1976). Unfortunately, CDOM is not easily quantified, making the terms C and P' difficult to define as functions of mass. CDOM concentration, C_{CDOM} , is therefore defined as a dimensionless dilution factor bounded by 0 and 1, where 1 is the source concentration within the SFE and P' is the value of absorption at a reference wavelength, $\lambda_o = 489$ nm, at source concentration, $a_{CDOM,489}^s$ m⁻¹. Spectrally, a_{CDOM} increases exponentially towards the blue and \mathcal{F}_{CDOM} can be accurately described as

$$\mathcal{F}_{CDOM} = e^{S_g(\lambda_0 - \lambda)}, \quad (10)$$

where $S_g \text{ nm}^{-1}$ is the spectral slope of a_{CDOM} in log space. In the open ocean, local microbial processes are believed to be the primary sources of CDOM while the majority of coastal and inland CDOM is of terrestrial origin, transported by streams and rivers (Babin et al., 2003). Reported values of S_g for coastal and inland waters are generally within the range 0.013 - 0.018 nm^{-1} .

3. RESULTS

In situ optical properties are assessed for accuracy through a test of closure with independent measurements of water reflectance, $R_w = f[b_b/(a + b_b)]$. If modeled values of reflectance, $[R_w]_{mod}$ agree with simultaneously observed water reflectance, $[R_w]_{obs}$, it may be concluded that the observed optical properties necessary to model reflectance, i.e., a , b , and \tilde{b}_b , are of reasonable accuracy. Water reflectance is computed for each data set using HydroLight (HL), a commercially available, radiance based radiative transfer model (Mobley and Sundman, 2008). HL computes the complete radiance distribution of the in-water and reflected light field for specified water optical properties and

environmental conditions. For each location, values of a , b , and \tilde{b}_b are averaged over a 20 min time series measured at each station and assumed to represent the upper portion of the water column contributing to R_w . HL is used to compute the above-surface water reflectance in the observation direction that R_w was measured with using a hand held spectrometer (135° azimuth relative to the sun and 40° nadir). The form of β is computed by constraining the Fournier-Forand formulation for the volume scattering function (Fournier and Forand, 1994) with measured values of \tilde{b}_b . Modeled reflectance, $[R_{s,w}]_{mod}$, is in agreement with observed values, $[R_{s,w}]_{obs}$ (Fig. 2). The linear correlation for all wavelengths is $r^2 = 0.88$, $N = 27$, and the mean relative error, $MRE = 100 * ([R_w]_{mod} - [R_w]_{obs})/[R_w]_{obs}$, for all wavelengths is $3.5\% \pm 4.5\%$. Spectrally, $MRE = 5.9\% \pm 9.1\%$ at $\lambda = 472 \text{ nm}$, $MRE = -1.5\% \pm 7.1\%$ at $\lambda = 526 \text{ nm}$, and $MRE = 6.0\% \pm 7.1\%$ at $\lambda = 654 \text{ nm}$.

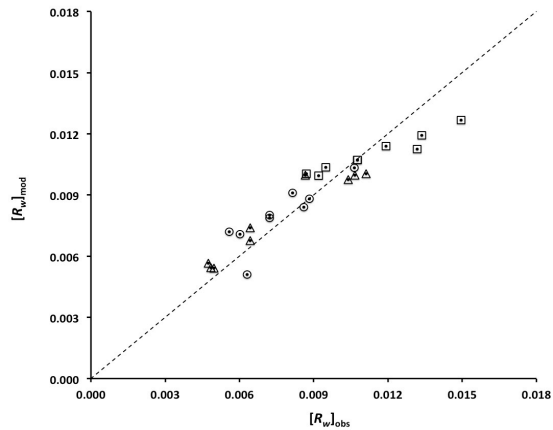


Figure 2. Comparison of observed ($[R_w]_{obs}$) and modeled ($[R_w]_{mod}$) water reflectance at 472 nm (circles), 526 nm (squares), and 654 nm (triangles) representing selected RIOSFE stations (see text). The dashed line represents perfect 1:1 agreement.

The water constituent parameters that comprise SFE-O, described in Section 2, are constrained with field measurements and summarized in Table 1.

The constituent-based model, where a and b are determined based on C_{chl} , C_{SPM} , and direct measurements of $a_{CDOM,488}$, is used to constrain HL to predict water reflectance and the in-water light field at each station. The results are compared with independent measurements of R_w (from above-water radiometry) and $Z_{PAR,1\%}$ (from the the rosette PAR sensor). The form of β was computed by constraining the Fournier-Forand formulation for the volume scattering

function (Fournier and Forand, 1994) with modeled values of \tilde{b}_p . Seven wavelengths spread across the visible spectrum are considered; $\lambda = 400$ nm, 450 nm, 500 nm, 550 nm, 600 nm, 650 nm, and 700 nm. Modeled water reflectance, $[R_w]_{\text{mod}}$, underestimates observed values, $[R_w]_{\text{obs}}$, by as much as 44% and overestimates by a maximum of 134% (Fig. 3). MRE ranges from -19% at 500 nm to 8% at 450 nm and is generally larger in the blue portion of the spectrum than in the red portion. This is most likely due to the fact that uncertainty in the spectral shape functions for SPM and CDOM are larger in the blue portion of the spectrum. This is to be expected since uncertainty in SPM and CDOM absorption is greatest at shorter wavelengths.

Table 1. Optical Model Constituent Parameter Definitions

| Constituent | P | $=$ | C | $*$ | P' | $*$ | \mathcal{F} |
|---------------|--------------------|-----|--|-----|--|-----|---|
| Phytoplankton | $a_{phy,\lambda}$ | | $C_{chl} \text{ mg m}^{-3}$ | | $a'_{chl,675} = 0.013 \text{ m}^2 \text{ mg}^{-1}$ | | $\frac{a_{chl,\lambda}}{a_{chl,675}}$ (Stramski, 2002) |
| | $b_{phy,\lambda}$ | | | | $b'_{chl,675} = 0.125 \text{ m}^2 \text{ mg}^{-1}$ | | $\frac{b_{chl,\lambda}}{b_{chl,675}}$ (Stramski, 2002) |
| SPM | $a_{SPM,\lambda}$ | | $C_{SPM} \text{ g m}^{-3}$ | | $a'_{SPM,489} = 0.049 \text{ m}^2 \text{ g}^{-1}$ | | $\sum_0^3 x_i [\lambda/\lambda_o]^i$ 400 nm $\leq \lambda \leq$ 750 nm $\lambda_o = 489$ nm $x_0 = 19.741$ $x_1 = -43.174$ $x_2 = 32.864$ $x_3 = -8.428$ ----- $\sum_0^3 x_i [700/\lambda_o]^i$ $\lambda > 750$ nm |
| | $b_{SPM,\lambda}$ | | | | $b'_{SPM,652} = 0.417 \text{ m}^2 \text{ g}^{-1}$ | | $\left[\frac{\lambda}{\lambda_o}\right]^{-\eta}$ $\lambda_o = 652$ nm $\eta = 0.675$ |
| CDOM | $a_{CDOM,\lambda}$ | | $a_{CDOM,489}/a_{CDOM,489}^s$ $0 \leq C \leq 1$ | | $a_{CDOM,489}^{max}$ | | $exp^{S_g(\lambda_o-\lambda)}$ $S_g = 0.0165 \text{ nm}^{-1}$ $\lambda_o = 489$ nm |

PAR is modeled as a function of depth:

$$PAR(z) = \frac{1}{hc} \sum_{\lambda=400}^{700,50} \lambda E_{o,\lambda}(0-) exp^{-K_{o,\lambda}z} \mu\text{mol m}^{-2} \text{ s}^{-1}, \quad (11)$$

where c is the speed of light and h is Planck's constant and $E_{o,\lambda}(0-)$ W m^{-2} is the spectrum of solar irradiance occurring just below the water surface under a clear sky. The modeled values of

$PAR(z)$ are then use to estimate K_{PAR} using a least-squares regression between $\ln[PAR(z)]$ and z and the 1% PAR depth computed as

$$z_{1\%PAR} = -\ln(0.01)/K_{PAR}. \quad (12)$$

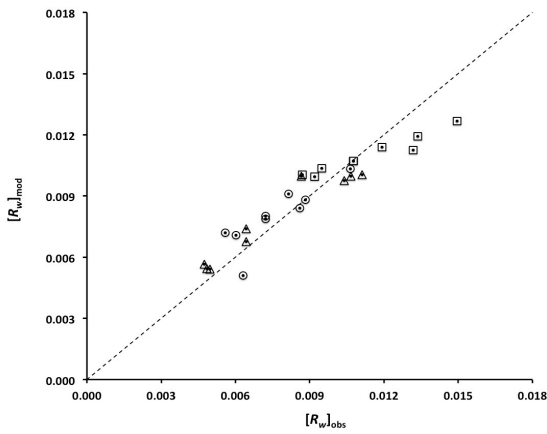


Figure 3. Comparison of observed ($[R_w]_{obs}$) and modeled ($[R_w]_{mod}$) water reflectance at 472 nm (circles), 526 nm (squares), and 654 nm (triangles) representing selected RIOSFE stations (see text). The dashed line represents perfect 1:1 agreement.

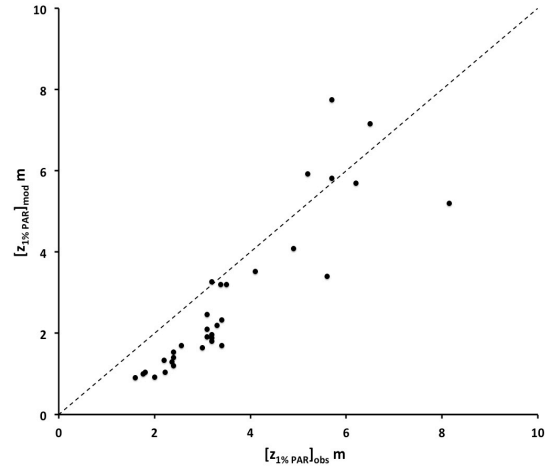


Figure 4. Observed (subscript "obs") versus modeled (subscript "mod") depth of the 1% surface PAR. The dashed line represents perfect 1:1 agreement.

Modeled values, $[z_{1\%PAR}]_{mod}$, are positively correlated with measured values, $[z_{1\%PAR}]_{obs}$, $r^2 = 0.79$, $N = 33$, $MRE = -25.5 \pm 9.1\%$ (Fig. 4). Model underestimation occurs primarily where $z_{1\%PAR} < 4$ m. In other words, where absorption and turbidity conspire to reduce the penetration of PAR. Considering only data where $z_{1\%PAR} > 4$ m, the average relative error decreases to $2.9 \pm 16.2\%$. The increase in uncertainty with attenuation is likely due to the effects of ship shadow on measured in-water PAR (Voss et al., 1986; Piskozub, 2004). Therefore, PAR(0-) likely underestimated at higher turbidity relative to light levels lower down in the water column that would likely be less impacted by shadow. This would have the effect of overestimating the observed depth of 1% surface PAR.

4. CONCLUSIONS

The SFE-O optical model describes with reasonable accuracy the effects of suspended sediments, phytoplankton, and dissolved organic matter on the in-water light field and spectral reflectance of waters within the northern portions of San Francisco Bay, including the Delta and lower reaches of the Sacramento River. The conditions under which the model is constructed represent extreme drought conditions, as were observed in 2014 and 2015. While the environment is optically challenging, a test of closure between measured optical properties, good agreement between measured optical signals and water constituent concentration, and reasonable agreement between the predicted and observed optical environment based on constituent concentration indicate that the field observations are of high quality. The resulting optical model should prove helpful in understanding the near-term conditions of the SFE and to evaluate potential future change resulting from population and climate.

5. REFERENCES

- ABAG. 2015. San Francisco Bay Area state of the region; Economy, population, housing; 2015. Association of Bay Area Governments, ABAG Publication P15001PRO.
- Babin, M., D. Stramski, G. M. Ferrari, H. Claustre, A. Bricaud, G. Obolensky, and N. Hoepffner. 2003. Variations in the light absorption coefficients of phytoplankton, nonalgal particles, and dissolved organic matter in coastal waters around Europe. *J. Geophys. Res.*, 108(C7):3211, doi:10.1029/2001JC000882.
- Ciotti, Á. M., M. R. Lewis, and J. J. Cullen. 2002. Assessment of the relationships between dominant cell size in natural phytoplankton communities and the spectral shape of the absorption coefficient. *Limnol. Oceanogr.*, 47(2):404-417.
- Cloern, J.E., N. Knowles, L. R. Brown, D. Cayan, M. D. Dettinger, T. L. Morgan, D. H. Schoellhamer, M. T. Stacey, M. van der Wagen, R. W. Wagner, and A. D. Jassby. 2011. Projected Evolution of California's San Francisco Bay-Delta-River System in a Century of Climate Change. *PLoS ONE* 6(9): e24465, doi:10.1371/journal.pone.0024465.
- Fournier, G. R. and J. L. Forand. 1994. Analytic phase function for ocean water," *SPIE*, Vol.2258, *Ocean Optics XII*, J. S. Jaffe, ed., pp. 194-201.
- Jerlov, N. G. 1976. *Marine Optics*. Elsevier Oceanography Series, 5. New York. 231 p.
- Mobley, C.D., & Sundman, L.K. (2008). *Hydrolight 5 Ecolight 5 Users' Guide*. Bellvue, WA, USA: Sequoia Scientific.
- Murrell, M. C. and J. T. Hollibaugh. 2000. Distribution and Composition of Dissolved and Particulate Organic Carbon in Northern San Francisco Bay During Low Flow Conditions. *Estuarine, Coast and Shelf Sci.*, 51:75-90, doi:10.1006/ecss.2000.0639.
- Müller-Solger, A. B., A. D. Jassby, and D. C. Müller-Navarra. 2002. Nutritional quality of food resources for zooplankton (*Daphnia*) in a tidal freshwater system (Sacramento–San Joaquin River Delta). *Limnol. Oceanogr.*, 47(5):1468-1476.
- Piskozub, J. 2004. Effect of ship shadow on in-water irradiance measurements. *Oceanologia*, 46(1):103-112.
- Schoellhamer, D.H. 2002. Variability of suspended-sediment concentration at tidal to annual time scales in San Francisco Bay, USA. *Cont. Shelf Res.*, 22:1857-1866.
- Service, R. F. 2007. Environmental restoration: Delta blues, California style. *Sci.*, 317: 442–445, doi: 10.1126/science.317.5837.442.
- Stramski, D., A. Bricaud, and A. Morel. 2001. Modeling the inherent optical properties of the ocean based on the detailed composition of the planktonic community. *Appl. Opt.*, 40(18):2929-2945.
- Voss, K. J., J. W. Nolten, and G. D. Edwards. 1986. Ship shadow effects on apparent optical properties. *SPIE, Ocean optics VIII*, 637:186-190.